

Dalton Transactions

Accepted Manuscript



This is an *Accepted Manuscript*, which has been through the Royal Society of Chemistry peer review process and has been accepted for publication.

Accepted Manuscripts are published online shortly after acceptance, before technical editing, formatting and proof reading. Using this free service, authors can make their results available to the community, in citable form, before we publish the edited article. We will replace this *Accepted Manuscript* with the edited and formatted *Advance Article* as soon as it is available.

You can find more information about *Accepted Manuscripts* in the [Information for Authors](#).

Please note that technical editing may introduce minor changes to the text and/or graphics, which may alter content. The journal's standard [Terms & Conditions](#) and the [Ethical guidelines](#) still apply. In no event shall the Royal Society of Chemistry be held responsible for any errors or omissions in this *Accepted Manuscript* or any consequences arising from the use of any information it contains.

One-Pot Synthesis of M (M= Ag, Au)@SiO₂ Yolk-Shell Structure via Organosilane-Assisted Method: Preparation, Formation Mechanism and Application in Heterogeneous Catalysis

Yu Chen,^{a,b} Qihua Wang^{*a} Tingmei Wang,^a

^a State Key Laboratory of Solid Lubrication, Lanzhou Institute of Chemical Physics, Chinese Academy of Sciences, Lanzhou, 730000, P. R. China.

^b University of Chinese Academy of Sciences, Beijing, 100039, P. R. China.

Abstract

We demonstrate the fabrication of yolk-shell catalyst of single M (M= Ag, Au) nanoparticle encapsulated within hollow mesoporous organosilica shell via an organosilane-assisted strategy. The advantages of our method lie in its good controllability of the void space as well as the thickness of mesoporous shell. The M@CTAB/SiO₂ synthesized through a modified Stöber method can transform to yolk-shell structures after adding (3-Aminopropyl)trimethoxysilane (APTMS) / TEOS or (3-Aminopropyl)triethoxysilane (APTES) / TEOS into the synthetic medium. We give unambiguous indication that the middle CTAB/SiO₂ layer transform into a less dense APTMS-rich organic-inorganic layer which was selectively removed in alkaline aqueous solution, while the amino-functionalized hybrid shells remain intact. Moreover, we discuss about the role of alkylamino groups in the shell for the transformation from Ag@SiO₂ nanorattles to hollow structures when impregnating the as-synthesized Ag@SiO₂ nanorattles in HAuCl₄ aqueous solution. The nanorattles also exhibit high catalytic activity for the catalytic reduction of p-nitrophenol.

Keywords: *one-pot synthesis, organosilane-assisted selective etching, yolk-shell, mesoporous, silica*

Introduction

Hollow structures are powerful platform in many important research fields, including drug carriers,¹⁻³ building blocks of photonic crystals,⁴⁻⁷ and as vessels for confined reaction.⁸⁻¹² An important aspect about hollow colloidal particles is that the so-called yolk-shell or rattle-type nanocomposites with diverse properties could be achieved by encapsulating different core materials.^{13,14} The integration of mesoporous silica spheres with functional metal nanoparticles (such as Ag, Au) to form yolk-shell nanostructures attract an increasing attention because of their great potential for application in various fields, such as nanoreactors,¹⁵⁻¹⁷ medical imaging.¹⁸⁻²⁰ A typical route of synthesizing yolk-shell structures is template-assisted approach, in which double-coat different materials on presynthesized core materials and the middle shell is selectively removed by either thermal decomposition or chemical dissolution. However, the preparation and removal procedures of the sacrificial template are often complicated, uneconomic and tedious. Recently, some progress in the synthesis of rattle-type structures has been achieved, such as soft template,²¹⁻²⁴ Ostwald ripening process²⁵ and other method.²⁶⁻³⁰

Very recently, the uniform silica spheres, derived from the Stöber method, are confronting growing signs that the external and internal structures are inhomogeneous.^{31,32} The residual groups $-R_1$ ($R_1 = -OCH_2CH_3$ or $-OH$) as structural defects mainly distribute in inner section of silica which provide more porous and less dense structures than the outmost shell. The structural difference also provides enormous opportunities for the development of silica-based materials with new structures and functionalities. But the utilization of internal defects is often difficult and passive. A significantly increasing number of silicon atoms fully coordinated to nearest neighbours of other silicates would occur in high temperature, thereby reducing the difference on structures of core and shell. Therefore, it is highly valuable to change the intrinsic nature of $-Si-O-Si-$ framework of silica nanoparticles. Notably, Tang et al.^{33,34} reported a designed “sandwich” structure which the middle organic-inorganic hybrid layer can be selectively removed with an appropriate amount of aqueous hydrofluoric acid (HF). However, the strategy still need the presynthesized core/shell structures. Moreover, the core and shell are made of the same materials which limit the practical applications.

Herein, we present an a facile and effective method for the fabrication of $M@SiO_2$ nanorattles with amino-functionalized mesoporous hybrid shell by an organosilane-assisted selective etching strategy. Compared with previous methods used for preparing yolk/shell structures, the advantages of our method lie in its good controllability of the void space as well as the thickness of mesoporous shell. The important role of organosilane precursors (such as APTMS or APTES) for the structure evolution from core-shell structured $M@CTAB/SiO_2$ to $M@SiO_2$ nanorattles was confirm. Moreover, we try to discuss about the role of alkylamino groups in the shell for the transformation from $Ag@SiO_2$ nanorattles

to hollow silica structures when impregnating the as-synthesized Ag@SiO₂ nanorattles in HAuCl₄ aqueous solution. Finally, we also demonstrate that the designed nanorattles can be used as a nanoreactor by using catalytic reduction of 4-nitrophenol as a model reaction.

Experimental

Chemical and Regents. All materials were of analytical grade and used as received without any further purification. Hexadecyl trimethyl ammonium bromide (CTAB) and tetraethyl orthosilicate (TEOS) were purchased from Sigma. (3-aminopropyl)trimethoxysilane (APTMS), (3-aminopropyl)triethoxysilane (APTES) were purchased from Aladdin. Gold chloride, silver nitrate and Sodium hydroxide were purchased from Sinopharm Chemical Reagent Co., Ltd. Ultrapure water (18.25 MΩcm⁻¹) was obtained using a Nanopure System from aquapro International Company LLC.

Synthesis of yolk-shell structured nanocomposites with Ag and Au cores.

In a typical synthesis, 0.05 g of CTAB was dissolved in the solution containing 24 mL of water and 1 mL of 0.5 M NaOH. After stirring at 80 °C for 20 min, 0.3 mL of 1.0 M formaldehyde solution and 1.0 mL of 0.1 M silver nitrate aqueous solution were added. Then, a mixture of (0.1mL/0.2mL/0.3 mL) TEOS/ 2 mL ethanol was added with stirring. After stirring for 40 min, a mixture of 0.5 mL TEOS/(0.1mL/0.25mL/0.4mL) APTMS/ 2 mL ethanol was added with vigorous stirring. NaOH, which is used in the synthesis, not only act as a catalyst for sol-gel reaction, but also an etchant for structural evolution. The products were filtered after stirring for 12 h, washed by water and ethanol, and then dried at 50 °C in vacuum. To remove the surfactant, the as-synthesized products were dispersed in a solution of ethanol (120 mL) and ammonium nitrate (72 mg), and the mixture was heated at 60 °C for 3 h. Au@SiO₂ nanorattles can also be prepared when replacing the silver nitrate by gold chloride.

Transformation from Ag@SiO₂ nanorattles to hollow silica structures.

30 mg of Ag@SiO₂ nanorattles with amino-functionalized mesoporous hybrid shell was dispersed in 13 mL of HAuCl₄·3H₂O (1.9 mM / 7 mM / 14 mM) aqueous solution under stirring at 80 °C and hydrothermally treated for 2 h. After the mixture had cooled to room temperature, the mixture was centrifuged and washed three times with water.

Catalytic Reduction of *p*-nitrophenol (4-NP)

The reduction of 4-NP by NaBH₄ was chosen as a model reaction to test the catalytic activity of the catalysts. Typically, the reaction proceeded under room temperature conditions. 16.7 mL of 0.18 mmol L⁻¹ 4-NP was added to a mixture of 184 mg of NaBH₄ dispersed in 12.3 mL of ultrapure water. Then, a certain amount of the catalysts Au@SiO₂ yolk-shell structured nanocomposites were added into the above mixture under mixture. The mixture was kept stirring

and we took 2 ml of the mixture by pipette every 3 min. The samples were analyzed immediately on an UV-visible spectrometer. The concentration change of 4-NP was determined by the absorbance at its maximum peak. In the presence of catalysts, the absorption of 4-NP at 400 nm decrease along with a concomitant increase of the ~ 300 nm peak of p-aminophenol. The absorption spectra of the solution were measure in the range of 220~550 nm.

Characterization

X-ray diffraction (XRD) patterns were recorded on a Bruker D4 X-ray diffractometer with Ni-filtered Cu K α radiation (40 kV, 40 mA). Structural and morphological investigation of the products were performed by a JSM-6701F scanning electron microscope (SEM) and transmission electron microscope (TEM, Tecnai-G2-F30). The nitrogen sorption experiments were performed at 77 K using a Micromeritics ASAP Tristar 3000 system. The samples were degassed at 180 °C for 6 h on a vacuum line. The surface area and pore size were obtained by using Brunauer-Emmett-Teller (BET) and Barrett-Joyner-Halenda (BJH) methods, respectively. A Lambda 750 ultraviolet and visible (UV-vis) spectrophotometer was employed for the analysis of the 4-NP reduction.

Results and discussion

The synthetic procedure for the yolk-shell structures include three main steps, as shown in Figure 1a. After the *in situ* reduction of silver nitrate (chloroauric acid) by formaldehyde, the Ag nanoparticles were stabilized by surfactants CTAB in the alkaline aqueous solution. The next step involves in the preparation of the M@CTAB/SiO₂. Finally, the evolution from core-shell to yolk-shell structures occur after the addition of the mixture of organosilane/TEOS. NaOH here not only act as an catalyst for sol-gel reaction, but also the etchant. Ag@SiO₂, Au@SiO₂ yolk-shell structures have been successfully prepared (Figure 1b, Figure 1c). Each core material is encapsulated by a mesoporous shell with an average thickness of ~ 20 nm in which the core usually is not located in the center of the shell. The yolk-shell structures can also be prepared when replacing APTMS with APTES (Figure S1). To remove the surfactant, the as-synthesized products were dispersed in a solution of ethanol (120 mL) and ammonium nitrate (72 mg), and the mixture was heated at 60 °C for 3 h (Figure S2). Interestingly, when the hollow cavity increase, a blue-shift in the absorbance maxima of Ag@SiO₂ should be observed because of the lower dielectric constant materials (water). However, a red-shift in the absorbance maxima of Ag@SiO₂ was observed, which is attributed to the increase of average particle size (Figure S3). It is worth noting that the metallic nanoparticles encapsulated in hollow silica are not uniform. The formation of silver and gold metallic nanoparticles were also confirmed by X-ray powder diffraction (XRD) pattern. The wide-angle XRD pattern is shown in Figure 1d. From the patterns of silver and gold core nanorattles, four Ag or Au diffraction peaks can be seen at $2\theta = 38.15^\circ$ (38.27°), 44.37° (44.6°),

64.18° (64.68°), 77.55° (77.55°), assigned to (111), (200), (220) and (311) reflections of the cubic (fcc) silver and gold lattice, respectively, as well as a very broad signal at $2\theta = 22.31^\circ$ ascribed to amorphous silica, indicating the presence of crystalline Ag or Au in yolk/SiO₂ structures. The SEM image shows that the as-synthesized products is of highly uniform (Figure 1e). It is worth noting that the etching process does not depend on the presence of the core materials. Without core materials, hollow cavity can still obtain (Figure 1f). Note that, the average size of the Ag or Au particles encapsulated in hollow silica is smaller than 25 nm.

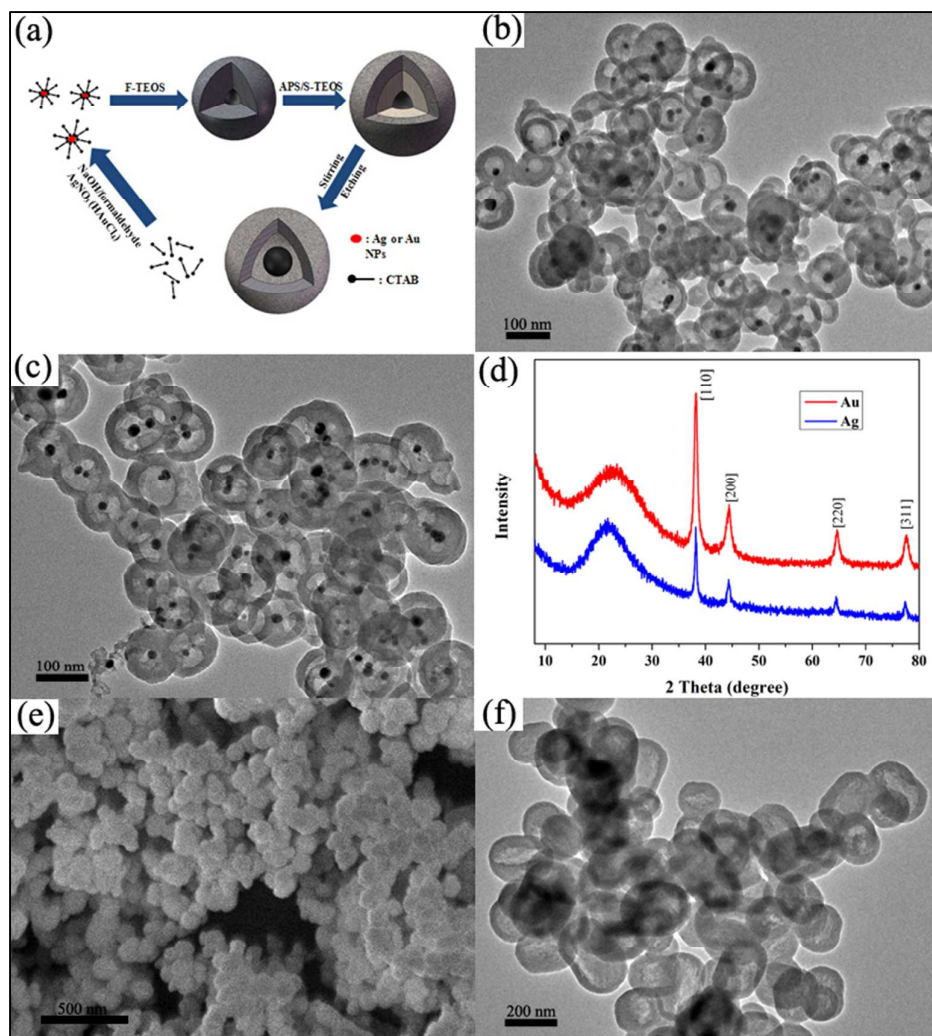


Figure 1. (a) Schematic illustrate of preparation process of the (Ag or Au)@SiO₂ nanorattles via the an organosilane-assisted selective etching strategy. TEM image of as-synthesized Ag@SiO₂ (b) and Au@SiO₂ (c) nanorattles. (d) Wide-angle XRD pattern of Ag@SiO₂ and Au@SiO₂ nanorattles. (e) SEM image of Ag@SiO₂ nanorattles. (f) TEM image of hollow structures.

The transformation, taking the formation process of Ag@SiO₂ nanorattles for example, was carefully monitored by TEM to detailed observe the formation mechanism of such yolk/shell structures. After the addition of TEOS (denoted as F-TEOS), the Ag@CTAB/SiO₂ particles

(Figure 2a) were first synthesized. Then, a mixture of APTMS/TEOS (denoted as S-TEOS) was added into the above solution. At the beginning of reaction, a “sandwich” structures was obtained. The middle CTAB/SiO₂ layer was slowly etched by NaOH and initially develop pores inside the silica matrix (Figure 2b). The selective etching of the middle layer is most likely a result of the relatively porous structures of middle layer. On the other hand, along with the introduction of APTMS, the role of CTAB for stabilizing the silicate against alkaline etching was broken because of the electrostatic interactions between -R₂ and CTAB. As the reaction proceeds, the middle layer began to collapse while the diameter of the nanocomposite remain constant (~90 nm) (Figure 2c). As etching time increases, those pores in the middle layer merge into a single void to reduce the surface energy. Finally, an evolution from core-shell to yolk-shell structures was observed (Figure 2d). The structure transformation process is depicted in Figure 2e. The as-synthesized nanorattles show a positive ζ potential as a result of the exist of amino groups in the organic-inorganic hybrid shell (Figure S4), which demonstrate the shells were co-condensed from the silicate and part of organosilane.

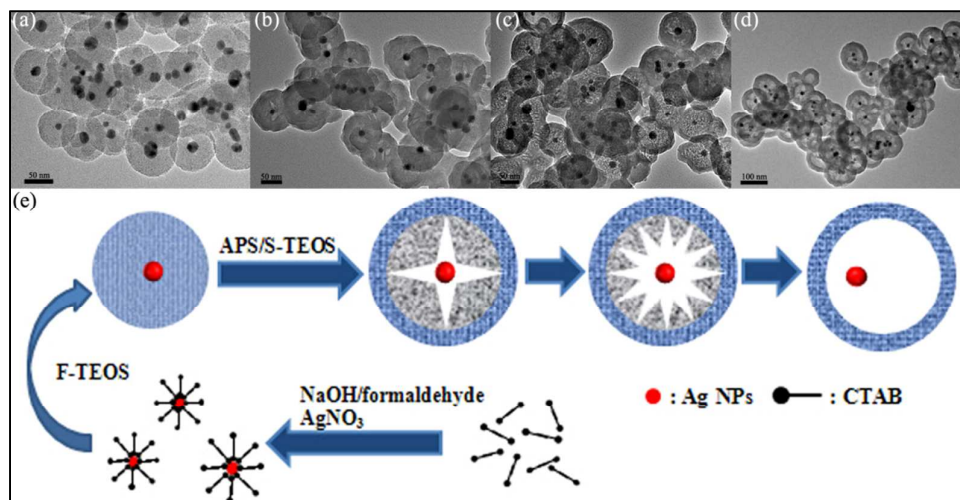


Figure 2. (a) TEM image of core-shell structured Ag@CTAB/SiO₂. TEM images of the Ag@SiO₂ nanorattles obtained at different times. (b) 1 hour, (c) 4 hour, (d) 12 hour. (e) The scheme of the formation process of Ag@SiO₂ nanorattles.

When varying the amount of F-TEOS, the volume of hollow cavity can be perfectly tailored from ~50 nm to ~100 nm (Figure 3a, Figure 3b), which demonstrate that the volume of hollow cavity is closely related with thickness of CTAB/SiO₂ layer. It is worth noting that the outer shell thickness decrease among with increasing the amount of F-TEOS, because a thicker middle layer should consume much more APTMS and S-TEOS thereby obtaining a thinner shell. After removing CTAB, the porosity of yolk/shell structures was investigated by N₂ adsorption-desorption measurements. The nitrogen sorption analysis results shown in Figure 3c, show a type II isotherm with H₄ hysteresis loop which is typical of hollow structures with mesoporous shell. The capillary condensation steps of the isotherms appearing in the relative pressure interval $P/P_0 = 0.2-0.4$ indicate that these materials has a

mesoporous structure with uniform pore size. The Barrett-Joyner-Halenda (BJH) pore size distribution curve further confirm the uniform mesopores size centered around 4 nm (Figure 3d). The Brunauer-Emmett-Teller (BET) specific surface area and volume are $57.25 \sim 81.8 \text{ m}^2\text{g}^{-1}$ and $0.156 \sim 0.188 \text{ cm}^3\text{g}^{-1}$. As we known, an organic-inorganic hybrid layer can be easily obtained via the hydrolysis and condensation of TEOS and organosiloxanes.^{32,33} Subsequently, the organic-inorganic layer can be easily selectively etched. Surprisingly, without the addition of F-TEOS, the yolk-shell structures cannot be prepared in our experiment. We attributed the reasons to the electrostatic interactions between CTAB and APTMS, which hinder the formation of organic-inorganic hybrid layer around the core materials. As a result, one part of silicate hydrolysed from S-TEOS form siloxane framework around the core materials (Figure 4a), meanwhile, some irregularly shaped silica matrix co-condensed from the residual silicate and APTMS were obtained (Figure 4b). Therefore, we realize that F-TEOS as a structure-directing agent play extremely important roles in the formation of organic-inorganic hybrid layer.

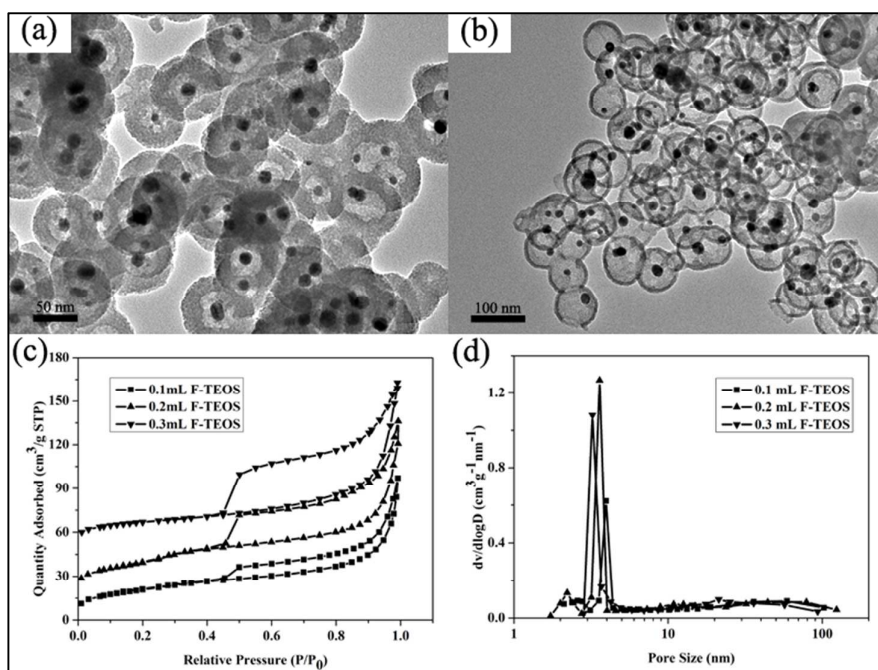


Figure 3. TEM image of Ag@SiO₂ nanorattles with different cavity volume (a) ~50 nm, (b) ~100 nm. The nitrogen sorption isotherm (c) and the pore size distribution curve (d) of the as-synthesized Ag@SiO₂ nanorattles with different cavity volume.

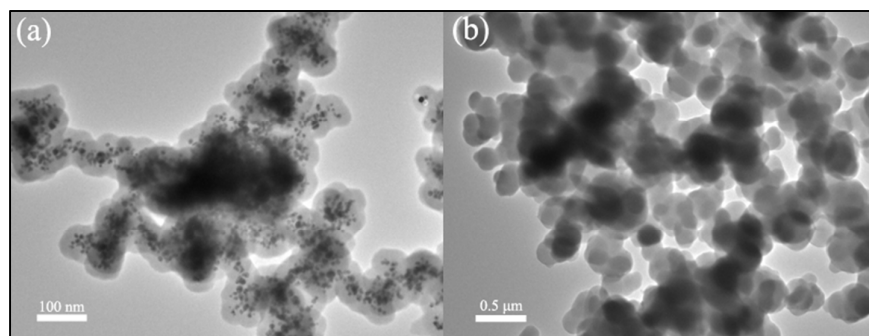


Figure 4. Without the F-TEOS involvement, the TEM images of the morphology of as-synthesized nanocomposite (a) and (b).

The thickness of shell can also be adjusted. When decreasing the amount of S-TEOS, a thinner shell (~ 10 nm) was observed as shown in Figure 5a. Without APTMS involvement, the residual $-R_1$ crosslink with each other in 80°C and the condensation degrees of the core by decomposing the Si-OH or Si-OCH₂CH₃ into Si-O-Si network were enhanced, consequently obtain a more compact inner structures which cannot be etched in slightly basic conditions (Figure 5b). Therefore, we hypothesized that organosilane (such as APTMS or APTES) play important role in destroying the hydrolysis and condensation balance of silica species thereby changing the intrinsic nature of $-\text{Si-O-Si}-$ framework of silica nanoparticles. While direct analysis of the role of organosilane remains challenging, we resort to detailed reactions to understand the mechanism. The effect of the concentration of APTMS to the yolk-shell structure was observed. When reducing the concentration of APTMS, a new type of particles was obtained (Figure 5c). The distinctive “sandwich” structures consist of a core, a middle porous layer and an outmost compact shell. A small amount of APTMS cannot destroy the hydrolysis and condensation balance of silica species and the role of CTAB for stabilizing the silicate against alkaline etching. However, an excessive amounts of APTMS brings negative effects on the formation of yolk-shell structures (Figure 5d). The reaction time of F-TEOS was also investigated to study the effects to final structures. When extending the reaction time of F-TEOS to 12 h, some irregularly shaped silica matrix are coexistent with yolk/shell particles as a result of the formation of more compact structures which greatly reduces the diffusion of APTMS (Figure S5). The above-described results give unambiguous indication that the middle CTAB/SiO₂ layer must transform into a less dense APTMS-rich organic-inorganic layer which was selectively removed in alkaline aqueous solution.

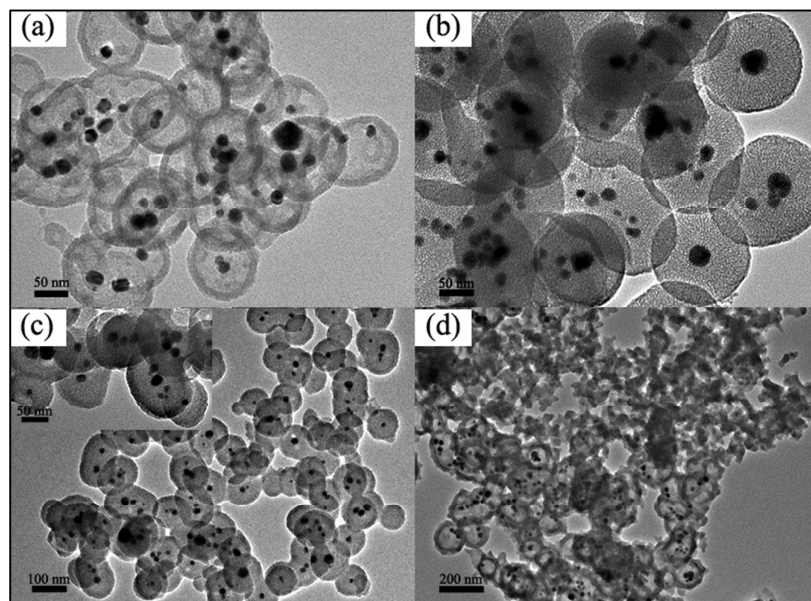


Figure 5. TEM image of (a) Ag@SiO₂ nanorattles with a 10-nm-thick shell, (b) Ag@CTAB/SiO₂, (c) distinctive “sandwich” structures, (d) Ag@SiO₂ nanocomposite.

On the basis of the above results, the evolution from core-shell to yolk-shell structures is depicted in Figure 6. After the addition of F-TEOS, the electrostatic interactions between silicate oligomers hydrolysed from TEOS and CTAB-stabilized core materials lead to the formation of core-shell structured M@CTAB/SiO₂. NaOH here not only act as a catalyst for sol-gel reactions, but also an etchant for structural evolution. Because of the short reaction time (40 min) of F-TEOS, F-TEOS hydrolyzed and condensed incompletely which rendered the CTAB/SiO₂ matrix less dense and more porous, as proven by ²⁹SiNMR characterization.³⁵ When adding a mixture of APTMS/S-TEOS into the above system, those groups -R₁ homogeneously distributed in the CTAB/SiO₂ matrix induce the inward diffusion of APTMS, in which Si-R₁ crosslinks with -R₂. It is worth noting that the hydrolyzed APTMS is more acidic and lower in concentration than the hydrolyzed TEOS in the mixture. Consequently, APTMS should be consumed before TEOS. Therefore, the middle APTMS-rich matrix was much more porous and less dense than the outmost shell via the hydrolysis and condensation of S-TEOS and residual APTMS. Afterward, the sodium hydroxide, which was used in the synthesis, will preferentially etch the less dense APTMS-rich silica matrix, while the shell remain intact.

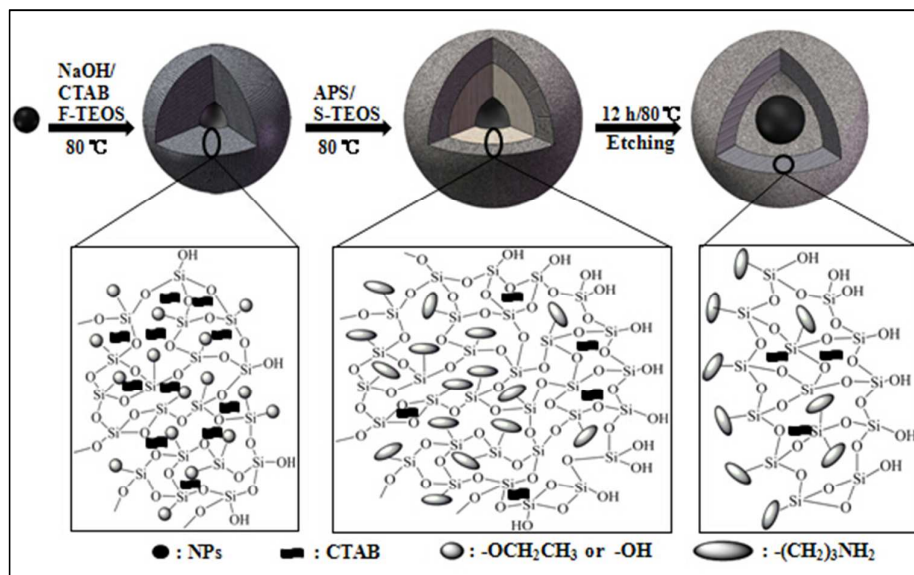


Figure 6. Schematic representation of the synthesis of Ag@SiO₂ nanorattles

As we know, a replacement reaction occur when impregnating Ag nanoparticles in HAuCl₄ aqueous solution thereby obtaining Ag-Au alloy or Au nanoparticles.^{36,37} However, different from the phenomenon reported before, a novel phenomenon was observed. After impregnating the as-synthesized Ag@SiO₂ nanorattles in HAuCl₄ aqueous solution, the color of the mixture changed from yellow to pink or purple during hydrothermal treatment. Observed from TEM images, to our surprised, most of Ag@SiO₂ nanorattles transform to hollow structure, while some cores in nanorattles were bigger than before (Figure S6a). When changing the HAuCl₄ concentration from 1.9 mM to 9 mM and 14 mM, much bigger cores were obtained (Figure S6b) and this can also be verified by the UV-vis absorbance in which the corresponding plasmon peaks red-shift from 535 nm to over 550 nm (Figure S6c). The disappearance of the adsorption peak of Ag@SiO₂ nanorattles is most likely due to the consumption of silver nanoparticles by AuCl₄⁻ ions. The elemental mapping by EDS analysis was carried out to further confirm the composition of metal nanoparticles (Figure S6d). The results show that the metal nanoparticles are gold. A very small amount of silver element mainly comes from the undissolved AgCl. According to the above-mentioned mechanism, the interior of the silica nanorattles have plenty of residual alkylamino groups. Therefore, we hypothesized that the alkylamino groups dispersed in mesoporous shell play important role in the transformation from nanorattles to hollow structures. One hand, the alkylamino groups could facilitate the newly generated Au seeds to diffuse in/out of the mesoporous shell before redeposit on Ag nanoparticles as a result of the electrostatic interaction between alkylamino groups and negative Au seeds. On the other hand, the alkylamino groups can act as in situ reducing agent for the growth of metal nanoparticles.³⁸ As a result, Ag nanoparticles should be consumed thereby obtaining hollow structures, while some Au nanoparticles encapsulated in nanorattles grow bigger. Further work needs to carried out in order to clarify the particular role of alkylamino groups.

In the following, we will demonstrate the successful incorporation of noble metal nanoparticles into the structure of mesoporous silica acting as a nanoreactor. From the UV-vis spectra (Figure 7a), a 9 nm red-shift in the maximum absorption peak of Au@SiO₂ nanorattles compared with that of bare Au nanoparticles was observed, which contribute to an increase in the local refractive index of mesoporous silica shell. To evaluate the catalytic performance of Au@SiO₂ nanorattles, we used a well-known model reaction, where p-nitrophenol was reduced to p-aminophenol using NaBH₄ as the reductant. Figure 7b shows the UV-vis spectra for the reduction of p-nitrophenol measured at a different time during the progress of the reaction. The absorption peak at 400 nm disappeared along with the appearance of the adsorption peak at 305 nm, indicating the formation of 4-aminophenol. The reaction was completed after 15 min. The ratio of C_t and C₀, where C_t is the concentration at time t and C₀ is the initial concentration, was measured from the relative intensity ratio of the respective absorbance at 400 nm. The linear relationship of ln(C_t/C₀) versus time was observed, indicating that the reactions followed first-order kinetics (Figure 7c). Furthermore, the nanoreactors can be easily recovered from the reaction solution by centrifugation and show excellent reusability. Compared to Au@SiO₂, the conversion of 4-NP by bare Au nanoparticles decreased quickly because of the irreversible aggregation (Figure 7d).

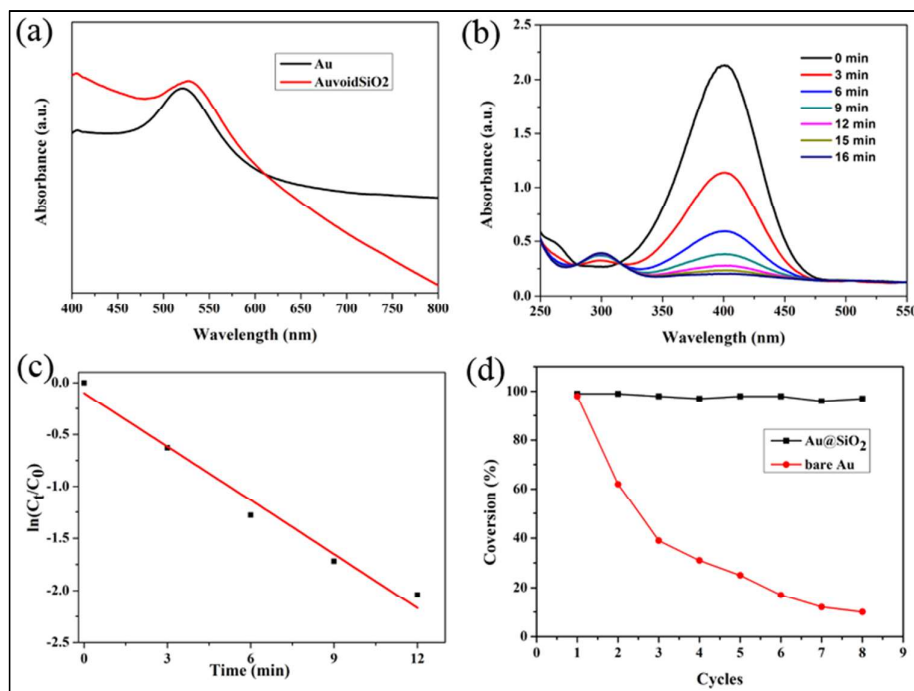


Figure 7. (a) UV-vis spectra of Au nanoparticles and Au@SiO₂ nanorattles. (b) Time-dependent UV-vis absorption spectral changes of the reaction catalyzed by Au@SiO₂ nanorattles. (c) plot of ln(C_t/C₀) versus time using Au@SiO₂ nanorattles as catalysts. (d) The reusability of the Au@mSiO₂ as catalysts.

Conclusions

In summary, we have developed a facile organosilane-assisted selective etching strategy to fabricate yolk-shell structures with tailored the void space, shell thickness and compositions of cores. The mechanism of the structure evolution from core-shell to yolk-shell is hypothesized,

in which the middle APTMS-rich organic-inorganic layer was selectively removed in alkaline aqueous solution because of their less compact structures. The yolk-shell nanocomposites with Au cores and organic-inorganic hybrid silica shells show high activity in the catalytic reduction of p- nitrophenol. This method may provide a general strategy to synthesize functional various type yolk-shell structured nanocomposites, which provide opportunities to yield a variety of applications, such as confined nanoreactors, drug delivery systems, as well as building blocks of photonic crystals.

ASSOCIATED CONTENT

Supporting Information

Experiment in detail; TEM image of Ag@SiO₂ nanorattles when replacing APTMS with APTES. The FT-IR spectra of as-made yolk-shell Ag@CTAB/SiO₂ before and after removing CTAB. The optical properties of Ag@SiO₂ fabricated with different amount of F-TEOS. The as-synthesized nanorattles show a positive ζ potential. The TEM images of the morphology of as-synthesized nanocomposite without the F-TEOS involvement. TEM image of Ag@SiO₂ nanorattles obtained by impregnating the as-synthesized Ag@SiO₂ nanorattles in different concentration of HAuCl₄ aqueous solution.

AUTHOR INFORMATION

Corresponding Author

*E-mail: wangqh@licp.cas.cn. Fax: +86-0931-4968180.

Notes

The authors declare no competing financial interest.

Acknowledgements

We greatly appreciate financial support from the National Science Foundation for Distinguished Young Scholars of China (grant no.51025517), the National Defense Basic Scientific Research Project (A1320110011) are duly acknowledged, the National Basic Research Program of China (973 Program, Grant No. 2015CB057502).

Notes and references

- (1) P. Yang, S. Gai, J. Lin, *Chemical Society reviews* **2012**, *41*, 3679.
- (2) I. I. Slowing, B. G. Trewyn, S. Giri, V. S. Y. Lin, *Adv. Fun. Mater.* **2007**, *17*, 1225.
- (3) J. Yang, D. Shen, L. Zhou, W. Li, X. Li, C. Yao, R. Wang, A. M. El-Toni, F. Zhang, D. Zhao, *Chem. Mater.* **2013**, *25*, 3030.
- (4) X. Xu, S. A. Asher, *J. Am. Chem. Soc.* **2004**, *126*, 7940.
- (5) J. Ge, Y. Hu, T. Zhang, Y. Yin, *J. Am. Chem. Soc.* **2007**, *129*, 8974.
- (6) Y. Liu, X. Han, L. He, Y. Yin, *Angew. Chem.* **2012**, *51*, 6373.
- (7) Y. Hu, L. He, Y. Yin, *Angew. Chem.* **2011**, *50*, 3747.

- (8) M. Chen, L. Wu, S. Zhou, B. You, *Adv. Mater.* **2006**, *18*, 801.
- (9) S. Wang, M. Zhang, W. Zhang, *ACS Catalysis* **2011**, *1*, 207.
- (10) K. Kamata, Y. Lu, Y. N. Xia, *J. Am. Chem. Soc.* **2003**, *125*, 2384.
- (11) Y. Yang, X. Liu, X. Li, J. Zhao, S. Bai, J. Liu, Q. Yang, *Angew. Chem.* **2012**, *51*, 9164.
- (12) H. S. Shin, S. Huh, *ACS Appl. Mater. Interfaces* **2012**, *4*, 6324.
- (13) C. R. Ghosh, S. Paria, *Chemical Reviews* **2012**, *112*, 2373.
- (14) A. Guerrero-Martínez, J. Pérez-Juste, L. M. Liz-Marzán, *Adv. Mater.* **2010**, *22*, 1182.
- (15) J. Lee, J. C. Park, H. Song, *Adv. Mater.* **2008**, *20*, 1523.
- (16) Y. Chen, Q. Wang, T. Wang, *Dalton transactions* **2013**, *42*, 13940.
- (17) J. Zhu, T. Sun, H. H. Hng, J. Ma, F. Y. C. Boey, X. Lou, H. Zhang, C. Xue, H. Chen, Q. Yan, *Chem. Mater.* **2009**, *21*, 3848.
- (18) Y. Chen, H. Chen, Y. Sun, Y. Zheng, D. Zeng, F. Li, S. Zhang, X. Wang, K. Zhang, M. Ma, Q. L. Zhang, J. Shi, *Angew. Chem.* **2011**, *123*, 12713.
- (19) Z. Teng, X. Su, B. Lee, C. Huang, Y. Liu, S. Wang, J. Wu, P. Xu, J. Sun, D. Shen, W. Li, G. Lu, *Chem. Mater.* **2014**, *26*, 5980.
- (20) M. Colombo, S. Carregal-Romero, M. F. Casula, L. Gutierrez, M. P. Morales, I. B. Bohm, J. T. Heverhagen, D. Prospero, W. J. Parak, *Chemical Society Reviews* **2012**, *41*, 4306.
- (21) X. J. Wu, D. S. Xu, *J. Am. Chem. Soc.* **2009**, *131*, 2774.
- (22) D. C. Niu, Z. Ma, Y. S. Li, J. L. Shi, *J. Am. Chem. Soc.* **2010**, *132*, 15144.
- (23) J. Liu, S. Z. Qiao, S. Budi Hartono, G. Q. Lu, *Angew. Chem.* **2010**, *49*, 4981.
- (24) Q. Yue, M. Wang, J. Wei, Y. Deng, T. Liu, R. Che, B. Tu, D. Zhao, *Angew. Chem.* **2012**, *51*, 10368.
- (25) H. C. Zeng, *Current Nanoscience* **2007**, *3*, 177.
- (26) K. Zhang, H. Chen, Y. Zheng, Y. Chen, M. Ma, X. Wang, L. Wang, D. Zeng, J. Shi, *J. Mater. Chem.* **2012**, *22*, 12553.
- (27) Z. Teng, X. Su, Y. Zheng, J. Sun, G. Chen, C. Tian, J. Wang, H. Li, Y. Zhao, G. Lu, *Chem. Mater.* **2013**, *25*, 98.
- (28) X. Fang, C. Chen, Z. Liu, P. Liu, N. Zheng, *Nanoscale* **2011**, *3*, 1632.
- (29) T. Zhang, J. Ge, Y. Hu, Q. Zhang, S. Aloni, Y. Yin, *Angew. Chem.* **2008**, *47*, 5806.
- (30) M. Roca, A. J. Haes, *Chem. Soc.* **2008**, *130*, 14273.
- (31) S. J. Park, Y. J. Kim, S. J. Park, *Langmuir* **2008**, *24*, 12134.
- (32) Y. J. Wong, L. Zhu, W. S. Teo, Y. W. Tan, Y. Yang, C. Wang, H. Chen, *J. Am. Chem. Soc.* **2011**, *133*, 11422.
- (33) L. Tan, D. Chen, H. Liu, F. Tang, *Adv. Mater.* **2010**, *22*, 4885.
- (34) D. Chen, L. Li, F. Tang, S. Qi, *Adv. Mater.* **2009**, *21*, 3804.
- (35) X. Liu, P. Wang, L. Zhang, J. Yang, C. Li, Q. Yang, *Chemistry – A European Journal* **2010**, *16*, 12727.
- (36) J. Yang, J. Y. Lee, H. P. Too, *J. Phys. Chem. B.* **2005**, *109*, 19208.
- (37) I. Srnova-Sloufova, F. Lednický, A. Gemperle, J. Gemperlova, *Langmuir* **2000**, *16*, 9928.
- (38) K. Zhang, H. R. Chen, Y. Y. Zheng, Y. Chen, M. Ma, X. Wang, L. J. Wang, D. P. Zeng, J. L. Shi, *Journal of Materials Chemistry.* **2012**, *22*, 12553.